

# Spin-wave dispersion and transition temperature in the cuprate antiferromagnet $\text{La}_2\text{CuO}_4$

M. Manojlović, M. Pavkov,\* M. Škrinjar, M. Pantić, D. Kapor, and S. Stojanović

*Department of Physics, Faculty of Sciences, University of Novi Sad, Trg D. Obradovića 4, Novi Sad, Serbia and Montenegro, Yugoslavia*

(Received 26 February 2003; revised manuscript received 21 May 2003; published 30 July 2003)

We have studied the spin-wave dispersion at low temperatures and the transition temperature ( $T_N$ ) of the spin- $\frac{1}{2}$  antiferromagnet and high- $T_C$  parent  $\text{La}_2\text{CuO}_4$ . The values of the in-plane exchange parameters (including first, second, and third nearest neighbors) are determined by an accurate fit to the recently experimentally observed in-plane spin-wave spectrum, obtained by the high-resolution inelastic neutron scattering performed on  $\text{La}_2\text{CuO}_4$  [Phys. Rev. Lett. **86**, 5377 (2001)]. The analysis of the Néel temperature shows that the in-plane spin anisotropy ( $\eta$ ) is much more significant than the three dimensionality, since  $T_N$  of the three-dimensional (3D)-antiferromagnet depends rather weakly on the value of the interlayer coupling ( $\lambda_\perp$ ). We obtain that the Néel temperature of the 3D-antiferromagnet varies only weakly within the very wide interval of  $\lambda_\perp$  and the Néel temperature of the anisotropic 2D ( $\eta \neq 0$ ,  $\lambda_\perp = 0$ ) antiferromagnet does not differ from the 3D value for the same  $\eta$ . These conclusions are valid for both tetragonal and orthorhombic structures. However,  $\eta$  dependence of  $T_N$  is essentially different: for  $\eta = 0$ ,  $T_N$  of the tetragonal structure becomes 0, while  $T_N$  of the orthorhombic structure remains finite. These results are valid within the frame of the Tyablikov approximation.

DOI: 10.1103/PhysRevB.68.014435

PACS number(s): 75.10.Jm, 75.30.Gw, 75.40.Gb, 74.72.Dn

## I. INTRODUCTION

The study of the magnetic and thermodynamic properties of the high- $T_C$  superconductor parent compound  $\text{La}_2\text{CuO}_4$ , which has been intensive in the last decade, is significant for, at least, two reasons. First, it has been noticed that in the undoped regime high- $T_C$  superconductors have some peculiar features, which are assumed to play an important role in the mechanism of their transition to superconductive phase. For that reason, a great attention is paid to understanding the undoped-state properties of the high- $T_C$  cuprates. Second,  $\text{La}_2\text{CuO}_4$  appears to be a very good approximation to the 2D  $S = \frac{1}{2}$  Heisenberg antiferromagnet (AF) and, therefore, it is interesting from the purely theoretical point of view.

The first model used for the description of the interactions among  $\text{Cu}^{2+}$  spins in  $\text{La}_2\text{CuO}_4$  was simple 2D Heisenberg model with nearest-neighbor (NN) interactions only. However, recent experiments carried out on  $\text{La}_2\text{CuO}_4$  (Ref. 1) have shown that complete description of the spin excitations in  $\text{La}_2\text{CuO}_4$  requires involving next neighbors, i.e., NNN- and NNNN-exchange couplings. In fact, experimentally obtained spin-wave spectrum in Ref. 1 shows dispersion along 2D AF Brillouin zone boundary which can be explained only by including NNN-exchange coupling between  $\text{Cu}^{2+}$  spins.

Our intention in this paper was not only to fit 2D spin-wave spectrum from Ref. 1, but also to check if the same parameters, using the same model, can give correct value for the phase transition temperature (the Néel temperature). We also tried to resolve the existing dilemma about the nature (ferromagnetic or antiferromagnetic) of the interaction between NNN and NNNN.

From the phase diagram of  $\text{La}_2\text{CuO}_4$ ,<sup>2</sup> it can be seen that below the tetragonal-orthorhombic structural phase transition temperature ( $T_{st} = 530$  K),  $\text{La}_2\text{CuO}_4$  crystallizes in the face-centered orthorhombic phase.<sup>3</sup> However, upon doping, the crystal structure of  $\text{La}_2\text{CuO}_4$  changes (Fig. 1) into body-centered tetragonal structure (so-called  $T$  structure),<sup>2</sup> which

also partially characterizes the superconductive phase, providing thus the reason why many authors consider the tetragonal structure even in the studies of the undoped  $\text{La}_2\text{CuO}_4$ . In this paper, the tetragonal phase of  $\text{La}_2\text{CuO}_4$  will be considered, but it will also be shown that the orthorhombic phase behaves in almost the same way (Appendix).

This paper is organized as follows. In Sec. II, we define the effective Hamiltonian and derive the spin-wave spectrum and the expressions for the magnetization and the Néel temperature, using the method of the spin Green functions (GF). Section III contains the analysis of our results both for low and high (close to  $T_N$ ) temperatures, i.e., we compare our spin-wave spectrum to that obtained experimentally and as another test we calculate the Néel temperature for the obtained values of exchange parameters. The consequences of the results are summarized in the concluding Sec. IV.

## II. SPIN-WAVE SPECTRUM: THE NÉEL TEMPERATURE

The initial point of our considerations is the effective spin Hamiltonian, referring to the orthorhombic phase of  $\text{La}_2\text{CuO}_4$ , written in the following form:<sup>4</sup>

$$\begin{aligned} \hat{H} = J & \left( \sum_{\langle i, \delta_1 \rangle} \vec{S}_i \cdot \vec{S}_{i+\delta_1} + \eta \sum_{\langle i, \delta_1 \rangle} S_i^z S_{i+\delta_1}^z + \lambda_2 \sum_{\langle i, \delta_2 \rangle} \vec{S}_i \cdot \vec{S}_{i+\delta_2} \right. \\ & + \lambda_3 \sum_{\langle i, \delta_3 \rangle} \vec{S}_i \cdot \vec{S}_{i+\delta_3} + \sum_{\langle i, \delta_{\perp j} \rangle} \lambda_{\perp j} \vec{S}_i \cdot \vec{S}_{i+\delta_{\perp j}} \\ & \left. + \lambda_{DM} \sum_{\langle i, \delta_1 \rangle} (-)^i \vec{a}_1 \cdot \vec{S}_i \times \vec{S}_{i+\delta_1} \right). \end{aligned} \quad (1)$$

Here,  $J$  describes NN in-plane exchange coupling;  $\lambda_2$  and  $\lambda_3$  ( $\lambda_i = J_i/J$ ,  $i = 2, 3$ ) describe NNN and NNNN in-plane exchange couplings and are equivalent ( $\lambda_2 = \lambda_3$ );<sup>1</sup>  $\eta$  represents the in-plane spin anisotropy; and  $\lambda_{\perp 1}$  and  $\lambda_{\perp 2}$  explicitly describe different interlayer couplings in the orthorhom-

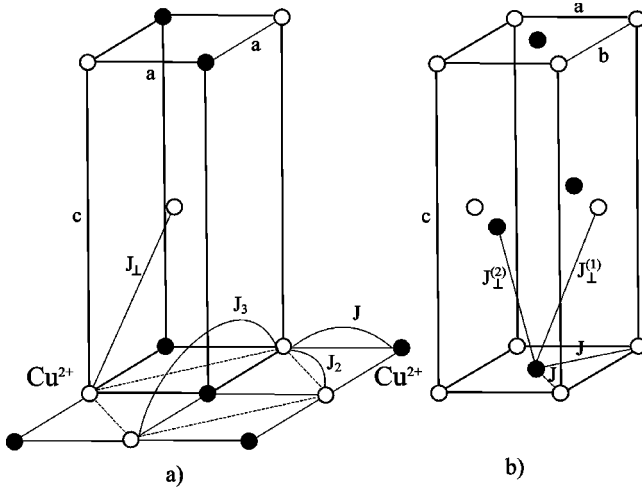


FIG. 1. Unit cell of the  $\text{La}_2\text{CuO}_4$  in (a) tetragonal and (b) orthorhombic phase with exchange interactions labelled.<sup>2</sup> Only  $\text{Cu}^{2+}$ -ions are shown. Two different orientations of spins are denoted by  $\circ$  and  $\bullet$ .

phase. The last term in Eq. (1) represents Dzyaloshinski-Moriya interaction, which describes a small rotation of  $\text{CuO}_6$  octahedra about the  $a$  axes, but can be neglected at low temperatures since it produces a very small gap in the Brillouin zone center.<sup>1,3</sup> On the other hand, this interaction vanishes due to symmetry in the tetragonal phase, while in the orthorhombic phase its influence at finite (close to transition) temperatures can also be neglected since there exist strong experimental evidence (Ref. 5 Sec. 3) that the system of coupled spins in  $\text{La}_2\text{CuO}_4$  is sufficiently well described by 2D Heisenberg model with the small anisotropy of the Ising type.

We shall consider here the tetragonal phase, when the Hamiltonian (1) simplifies since, as mentioned above,

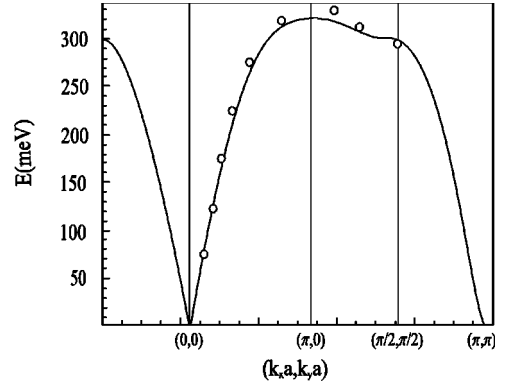


FIG. 2. Spin-wave dispersion in  $\text{La}_2\text{CuO}_4$  along the high symmetry directions in 2D AF Brillouin zone (for the tetragonal phase). The circles are the experimental results of Ref. 1 for  $\text{La}_2\text{CuO}_4$  at 10 K. The solid line is the result of a fit to the spin-wave dispersion result (19) leading to the exchange coupling constants given in Eq. (33).

Dzyaloshinski-Moriya interaction vanishes ( $\lambda_{DM}=0$ ) and the interlayer coupling becomes equivalent for all the out-of-plane NN ( $\lambda_{\perp 1}=\lambda_{\perp 2}$ ).

It can be also seen from Eq. (1) that the so-called ring (cyclic) exchange, considered by many authors<sup>1,6</sup> is not taken into account for reasons to be explained later.

In order to derive the spin-wave spectrum, we use the Tyablikov Green functions for the spin operators. Using the equations of motion for the following pairs of operators ( $\hat{S}^{+(a)}; \hat{S}^{-(b)}$ ) and ( $\hat{S}^{-(a)}; \hat{S}^{+(b)}$ ), we obtain, actually, due to the structure of the Hamiltonian, two independent systems of equations of motion for the Green functions, one of which is sufficient to derive all the relevant expressions. As an example, we quote here the equation of motion for GF  $\langle\langle \hat{S}_{m,\rho}^{+(a)} | \hat{B} \rangle\rangle_E$  in energy ( $E$ ) representation:

$$\begin{aligned}
E \langle\langle \hat{S}_{m,\rho}^{+(a)} | \hat{B} \rangle\rangle &= \frac{i}{2\pi} \langle [\hat{S}_{m,\rho}^{+(a)}, \hat{B}] \rangle + J \left( \sum_{\delta_1} \langle\langle \hat{S}_{m,\rho}^{z(a)} \hat{S}_{m,\rho+\delta_1}^{-(b)} | \hat{B} \rangle\rangle + (1+\eta) \langle\langle \hat{S}_{m,\rho+\delta_1}^{z(b)} \hat{S}_{m,\rho}^{+(a)} | \hat{B} \rangle\rangle \right) \\
&+ \lambda_{\perp} \sum_{\delta_{\perp}} \left( \langle\langle \hat{S}_{m,\rho}^{z(a)} \hat{S}_{(m,\rho)+\delta_{\perp}}^{+(a)} | \hat{B} \rangle\rangle - \langle\langle \hat{S}_{(m,\rho)+\delta_{\perp}}^{z(a)} \hat{S}_{m,\rho}^{+(a)} | \hat{B} \rangle\rangle + \langle\langle \hat{S}_{m,\rho}^{z(a)} \hat{S}_{(m,\rho)+\delta_{\perp}}^{-(b)} | \hat{B} \rangle\rangle + \langle\langle \hat{S}_{(m,\rho)+\delta_{\perp}}^{z(b)} \hat{S}_{m,\rho}^{+(a)} | \hat{B} \rangle\rangle \right) \\
&+ \lambda_2 \sum_{\delta_i} \left( \langle\langle \hat{S}_{m,\rho}^{z(a)} \hat{S}_{m,\rho+\delta_i}^{+(a)} | \hat{B} \rangle\rangle - \langle\langle \hat{S}_{m,\rho+\delta_i}^{z(a)} \hat{S}_{m,\rho}^{+(a)} | \hat{B} \rangle\rangle \right). \quad (2)
\end{aligned}$$

Here  $\hat{S}_{m,\rho}^{(\alpha)}$  denotes the spin of the  $\text{Cu}^{2+}$ -ion in the  $m$ th plane, the position within the plane is specified by  $\vec{\rho}$ , and  $\alpha=a,b$  refers to the sublattice.

The basic problem with the equations of type (2) is how to close the system by decoupling the higher-order Green functions. Close to the Néel temperature, one can use the Tyablikov decoupling approximation,<sup>7</sup> which is suitable for

that temperature region. Since this decoupling seems not to provide satisfying results at low temperatures (even for ferromagnets<sup>8</sup>), we use here a kind of modified Callen decoupling approximation, which is, for the particular case of spin  $\frac{1}{2}$  based on the identity

$$\hat{S}_g^z = S - \hat{S}_g^- \hat{S}_g^+ \quad (3)$$

In that case, the decoupling procedure for antiferromagnets is given in the following form:

$$\begin{aligned} \langle\langle \hat{S}_g^z \hat{S}_f^\pm | \hat{B} \rangle\rangle &\xrightarrow{g \neq f} S \left[ \left( 1 - \frac{1}{S} \langle \hat{S}_g^- \hat{S}_g^+ \rangle \right) \langle\langle \hat{S}_f^\pm | \hat{B} \rangle\rangle \right. \\ &\quad \left. - \frac{1}{S} \langle \hat{S}_g^\pm \hat{S}_f^\pm \rangle \langle\langle \hat{S}_g^\mp | \hat{B} \rangle\rangle \right], \end{aligned} \quad (4)$$

which enables the comparison to the boson approximation (e.g., Dyson-Maleev) and also makes possible better consideration of the quantum spin fluctuations in the antiferromagnetic ground state.

After decoupling and transforming to the momentum space, we obtain the following system of equations for GFs  $G_{aa}^{+-}(\vec{k}, E) = \langle\langle \hat{S}^{+(a)} | \hat{S}^{-(a)} \rangle\rangle_{\vec{k}, E}$  and  $G_{ba}^{--}(\vec{k}, E) = \langle\langle \hat{S}^{-(b)} | \hat{S}^{-(a)} \rangle\rangle_{\vec{k}, E}$ :

$$\begin{aligned} [E - JS\epsilon(\vec{k})]G_{aa}^{+-}(\vec{k}, E) - JSI(\vec{k})G_{ba}^{--}(\vec{k}, E) &= \frac{i}{2\pi} 2\langle \hat{S}^{z(a)} \rangle, \\ JSI(\vec{k})G_{aa}^{+-}(\vec{k}, E) + [E + JS\epsilon(\vec{k})]G_{ba}^{--}(\vec{k}, E) &= 0. \end{aligned} \quad (5)$$

Here the quantities  $\epsilon(\vec{k})$  and  $I(\vec{k})$  are given by the following expressions:

$$\begin{aligned} \epsilon(\vec{k}) &= z_1[(1 + \eta)(1 - \Phi) - \Phi_1] + \frac{z_\perp}{2}\lambda_\perp(1 - \Phi - \Phi_\perp^{ab}) \\ &\quad - \lambda_2\{z_2[1 - \gamma_2(\vec{k})](1 - \Phi + \Phi_2) + z_3[1 - \gamma_3(\vec{k})] \\ &\quad \times (1 - \Phi + \Phi_3)\} - \frac{z_\perp}{2}\lambda_\perp[1 - \gamma_\perp^{aa}(\vec{k})](1 - \Phi + \Phi_\perp^{aa}), \end{aligned} \quad (6)$$

$$\begin{aligned} I(\vec{k}) &= z_2\gamma_1(\vec{k})[1 - \Phi - (1 + \eta)\Phi_1] \\ &\quad + \frac{z_\perp}{2}\lambda_\perp\gamma_\perp^{ab}(\vec{k})(1 - \Phi - \Phi_\perp^{ab}), \end{aligned} \quad (7)$$

with the quantities  $\Phi$  given by

$$\Phi = \frac{1}{SN} \sum_{\vec{q}} \Phi^{-+}(\vec{q}), \quad (8)$$

$$\Phi_1 \equiv \frac{1}{SN} \sum_{\vec{q}} \gamma_\parallel(\vec{q})\Phi^{--}(\vec{q}), \quad (9)$$

$$\Phi_i \equiv \frac{1}{SN} \sum_{\vec{q}} \gamma_i(\vec{q})\Phi^{-+}(\vec{q}), \quad i=2,3, \quad (10)$$

$$\Phi_\perp^{aa} \equiv \frac{1}{SN} \sum_{\vec{q}} \gamma_\perp^{aa}(\vec{q})\Phi^{--}(\vec{q}), \quad (11)$$

$$\Phi_\perp^{ab} \equiv \frac{1}{SN} \sum_{\vec{q}} \gamma_\perp^{ab}(\vec{q})\Phi^{--}(\vec{q}), \quad (12)$$

where  $\Phi^{--}(\vec{q}) = \langle \hat{S}^- \hat{S}^- \rangle_{\vec{q}}$  and  $\Phi^{-+}(\vec{q}) = \langle \hat{S}^- \hat{S}^+ \rangle_{\vec{q}}$  are the correlation functions. The quantities  $\gamma(\vec{q})$  in tetragonal phase are given by

$$\gamma_1(\vec{q}) = \frac{1}{2}(\cos q_x a + \cos q_y a), \quad (13)$$

$$\gamma_2(\vec{q}) = \cos q_x a \cos q_y a, \quad (14)$$

$$\gamma_3(\vec{q}) = \frac{1}{2}(\cos 2q_x a + \cos 2q_y a), \quad (15)$$

$$\gamma_\perp^{aa}(\vec{q}) = \gamma_\perp^{bb}(\vec{q}) = \cos \frac{q_z c}{2} \cos \frac{a}{2}(q_x - q_y), \quad (16)$$

$$\gamma_\perp^{ab}(\vec{q}) = \gamma_\perp^{ba}(\vec{q}) = \cos \frac{q_z c}{2} \cos \frac{a}{2}(q_x + q_y). \quad (17)$$

The number of the corresponding neighbors is denoted by  $z_i$  ( $i=1,2,3,\perp$ ).

Spin-wave spectrum is obtained from system (5) in the form

$$E(\vec{k}) = JS \sqrt{\epsilon^2(\vec{k}) - I^2(\vec{k})} \equiv JS\omega(\vec{k}). \quad (18)$$

Since Ref. 1 gives the spin-wave spectrum of the 2D ( $\lambda_\perp = 0$ ) spin isotropic ( $\eta = 0$ ) model at low temperatures ( $T = 10$  K), in order to compare our expression to theirs, we use the following form of the energy of spin excitations:

$$\begin{aligned} E(\vec{k}; 0) &= 4JS[(1 - \Phi(0) - \Phi_1(0) - \lambda_2\{[1 - \gamma_2(\vec{k})] \\ &\quad \times [1 - \Phi(0) + \Phi_2(0)] + [1 - \gamma_3(\vec{k})][1 - \Phi(0) \\ &\quad + \Phi_3(0)\})]^2 - \gamma_1^2(\vec{k})[1 - \Phi(0) - \Phi_1(0)]^2]^{1/2}, \end{aligned} \quad (19)$$

where  $\Phi_i(0) \equiv \Phi_i(T=0)$ .

From Eq. (19) it can be seen that

$$\lim_{k \rightarrow 0} E(k) = 0,$$

which agrees with the fact that the spin isotropic magnets possess the Goldstone mode.

Solving Eq. (5), we arrive at the following expressions for the GFs:

$$G_{aa}^{+-}(\vec{k}, E) = \frac{i}{2\pi} 2\sigma \left( \frac{A(\vec{k})}{E - E(\vec{k})} + \frac{B(\vec{k})}{E + E(\vec{k})} \right), \quad (20)$$

$$G_{ba}^{--}(\vec{k}, E) = \frac{i}{2\pi} 2\sigma \left( \frac{C(\vec{k})}{E - E(\vec{k})} + \frac{D(\vec{k})}{E + E(\vec{k})} \right), \quad (21)$$

where

$$\sigma = \langle \hat{S}_z \rangle = S(1 - \Phi), \quad (22)$$

$$A(\vec{k}) = \frac{1}{2} + \frac{\epsilon(\vec{k})}{2\omega(\vec{k})}, \quad B(\vec{k}) = \frac{1}{2} - \frac{\epsilon(\vec{k})}{2\omega(\vec{k})},$$

$$C(\vec{k}) = -\frac{\epsilon(\vec{k})}{2\omega(\vec{k})}, \quad D(\vec{k}) = \frac{\epsilon(\vec{k})}{2\omega(\vec{k})}.$$

Using the standard procedure, we obtain the correlation functions, which figure in Eqs. (8)–(12):

$$\begin{aligned} \Phi^{-+}(\vec{k}) &= S(1-\Phi) \left( \frac{\epsilon(\vec{k})}{\omega(\vec{k})} - 1 \right) + 2S(1-\Phi) \\ &\times \frac{\epsilon(\vec{k})}{\omega(\vec{k})} \frac{1}{e^{E(\vec{k})/\theta} - 1}, \end{aligned} \quad (23)$$

$$\Phi^{--}(\vec{k}) = -S(1-\Phi) \frac{I(\vec{k})}{\omega(\vec{k})} - 2S(1-\Phi) \frac{I(\vec{k})}{\omega(\vec{k})} \frac{1}{e^{E(\vec{k})/\theta} - 1}. \quad (24)$$

The sublattice magnetization is given by the expression

$$\sigma = \frac{1}{2} - \frac{1}{N} \sum_{\vec{k}} \langle \hat{S}^- \hat{S}^+ \rangle_{\vec{k}}. \quad (25)$$

Inserting Eq. (23) in Eq. (25), we obtain the following expression:

$$\sigma = \frac{1}{2} \frac{1}{\frac{1}{N} \sum_{\vec{k}} \frac{\epsilon(\vec{k})}{\omega(\vec{k})} + \frac{2}{N} \sum_{\vec{k}} \frac{\epsilon(\vec{k})}{\omega(\vec{k})} \frac{1}{e^{E(\vec{k})/\theta} - 1}}. \quad (26)$$

In the case of spin isotropic magnet ( $\eta=0$ ), this expression for the sublattice magnetization is in agreement with Mermin-Wagner theorem.

In order to obtain the expression for the Néel temperature, we use the Tyablikov decoupling approximation [in Eqs. (6), (7), and (18) one needs to put  $\sigma=S(1-\Phi)$  and  $\Phi_i=0$ ,  $i=1,2,3,\perp$ ], which leads to the following expressions:

$$E(\vec{k}) = J\sigma \sqrt{[\epsilon^T(\vec{k})]^2 - [I^T(\vec{k})]^2}, \quad (27)$$

$$\begin{aligned} \epsilon^T(\vec{k}) &= z_1(1+\eta) + \frac{z_\perp}{2} \lambda_\perp - \lambda_2 \{z_2[1-\gamma_2(\vec{k})] \\ &+ z_3[1-\gamma_3(\vec{k})]\} - \frac{z_\perp}{2} \lambda_\perp [1-\gamma_\perp^{aa}(\vec{k})], \end{aligned} \quad (28)$$

$$I^T(\vec{k}) = z_2 \gamma_1(\vec{k}) + \frac{z_\perp}{2} \lambda_\perp \gamma_\perp^{ab}(\vec{k}). \quad (29)$$

Please notice that the contributions of the ferromagnetic (aa) coupling [Eq. (28)] and antiferromagnetic (ab) coupling [Eq. (29)], practically cancel in Eq. (27). Using Eqs. (27)–(29) and the fact that  $\sigma \rightarrow 0$  for  $T \rightarrow T_N$ , the Néel temperature can be expressed as

$$\theta_N = \frac{J}{C}, \quad (30)$$

where

$$C = \frac{1}{N} \sum_{\vec{k}} \frac{1 + \eta - \lambda_2 [2 - \gamma_2(\vec{k}) - \gamma_3(\vec{k})] + \lambda_\perp \gamma_\perp^{aa}(\vec{k})}{\{1 + \eta - \lambda_2 [2 - \gamma_2(\vec{k}) - \gamma_3(\vec{k})] + \lambda_\perp \gamma_\perp^{aa}(\vec{k})\}^2 - [\gamma_1(\vec{k}) + \lambda_\perp \gamma_\perp^{ab}(\vec{k})]^2}. \quad (31)$$

We shall now analyze these results.

### III. ANALYSIS OF THE RESULTS

We were able, by an accurate fit of our expression (19) to experimentally determined 2D spin-wave spectrum at 10 K,<sup>1</sup> to determine the system parameters  $J$  and  $\lambda_2$ . In order to evaluate these parameters, we applied the self-consistent procedure of determining the quantities  $\Phi$  [Eqs. (8)–(12)], which themselves depend on the energy. As a result, we obtained a set of parameters, which, as will be seen, leads to a correct description of the spin-wave spectrum in  $\text{La}_2\text{CuO}_4$  (Ref. 1) and also correctly reproduces the Néel temperature. The best fit is obtained for the following set of values:

$$\begin{aligned} \Phi &= 0.3469, \quad \Phi_1 = -0.6868, \quad \Phi_2 = 0.3879, \\ \Phi_3 &= 0.3012, \end{aligned} \quad (32)$$

which give

$$J = 141 \text{ meV} (\pm 5\%), \quad \lambda_2 = 0.0942 (\pm 10\%). \quad (33)$$

These values are very close to those given in Refs. 4 and 9.

The inelastic neutron scattering data from Ref. 1 together with our fit result along the high symmetry directions in the 2D AF Brillouin zone are shown in Fig. 2.

In the series of papers,<sup>1,6,10</sup> a valid fit of the spin-wave spectrum was obtained for different sets of parameters ( $J$ ,  $\lambda_2$ , and  $J_C$ ). The starting point of these studies was the Hubbard model ( $t$ - $U$  model, where  $t$  is the hopping energy between NN Cu sites and  $U$  is the potential energy on a given site;  $t/U \ll 1$ ), whose expansion produces the effective spin Hamiltonian with higher-order exchange terms, which arise from the coherent motion of the electrons beyond NN sites.<sup>11</sup> If the perturbation series is expanded to the order  $t^4$  (i.e., four hops), the effective Hamiltonian includes the following NN-, NNN-, and NNNN-exchange coupling constants:  $J = 4(t^2/U) - 24(t^4/U^3)$ ;  $J_2 = J_3 = 4(t^4/U^3)$ , and also the ring exchange  $J_C = 80(t^4/U^3)$ .

In Ref. 1, a valid fit of the spin-wave spectrum at 10 K is obtained in two ways. First, the spin-wave spectrum is fitted with the parameters  $J = 104 \pm 4$  meV;  $J_2 = -18 \pm 3$  meV (i.e., for ferromagnetic NNN interaction);  $J_3 = J_C = 0$ . Since

TABLE I. Néel temperature ( $T_N$ ) dependence on  $\lambda_\perp$  for  $\eta=9 \times 10^{-4}$  in tetragonal phase.

$\lambda_\perp$	$5 \times 10^{-5}$	$10^{-4}$	$10^{-3}$	$10^{-2}$	$10^{-1}$	0 (2D)
$T_N$ (K)	325	325	325.3	327.3	346.7	325

$J_2 < 0$  contradicts some theoretical predictions,<sup>1,12</sup> which give an antiferromagnetic NNN-exchange coupling constant ( $J_2 > 0$ ), another fit is presented in Ref. 1, using the spin Hamiltonian obtained by an expansion of the Hubbard Hamiltonian for  $t = 0.30 \pm 0.02$  eV and  $U = 2.2 \pm 0.4$  eV, which yields the following exchange constants:  $J = 146.3 \pm 4$  meV;  $J_2 = J_3 = 2 \pm 0.5$  meV;  $J_C = 61 \pm 8$  meV. Fit obtained with this set of parameters is also valid, yet it is indistinguishable from the previous one, obtained for the ferromagnetic  $J_2$ . This is the consequence of the fact that  $J_C$  actually reduces the interaction between NN ( $J - J_C/2 \approx 110$  meV) and the NNN-exchange coupling transfers to the ferromagnetic one ( $J_2 - J_C/4 \approx -14$  meV). Moreover, rather complicated exact expression for the equation of motion for  $\hat{S}^+$  in terms of spin operators indicates that in any relevant approximation (Tyablikov, Callen, etc.) the term with  $J_C$  will be proportional to  $\langle \hat{S}^z \rangle^3$ , i.e., in the expression for the magnon energy  $J_C$  is renormalized by  $\langle \hat{S}^z \rangle^2$ . In the vicinity of the phase transition temperature ( $\sigma \rightarrow 0$ ), this can always be neglected.

The fact that the experimental spin-wave spectrum can be fitted either with antiferromagnetic ( $J_2 > 0$ ) or with ferromagnetic ( $J_2 < 0$ ) NNN-exchange coupling, points to the necessity of another, independent test of the above results. For that reason, we calculated the Néel temperature [using Eqs. (30) and (31)] with the above-mentioned set of parameters [ $J = 141$  meV ( $\pm 5\%$ );  $\lambda_2 = 0.0942$  ( $\pm 10\%$ )] for different values of  $\lambda_\perp$  and  $\eta$ .

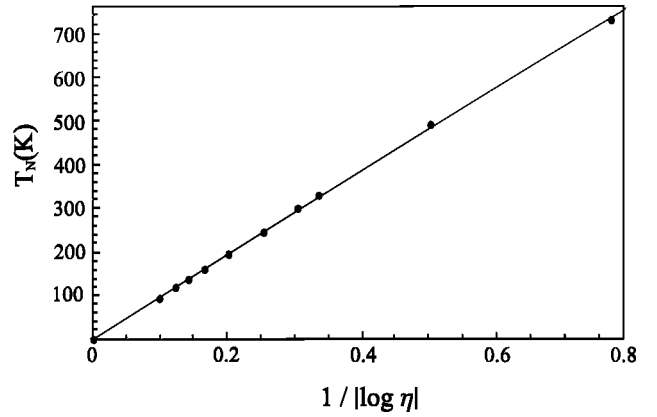
First, the Néel temperatures were calculated for fixed  $\eta$ , varying only  $\lambda_\perp$ , in order to examine the influence of the interlayer coupling. For the parameter  $\eta$ , we take the value  $\eta \approx 10^{-3}$ , which gives the best agreement with the experimental value  $T_N = 325 \pm 5$  K.<sup>4,9,13</sup> The results obtained are shown in Table I.

The results from Table I show the following: for fixed  $\eta$ ,  $T_N$  varies only weakly within the very wide interval of  $\lambda_\perp$  ( $10^{-5} - 10^{-2}$ ). Even in 2D-case ( $\lambda_\perp = 0$ ),  $T_N$  almost does not differ from its 3D value. We see that the influence of the interlayer coupling becomes significant only for  $\lambda_\perp > 10^{-1}$ , which is not characteristic for these systems.

In order to examine the influence of the spin anisotropy, we also calculated the Néel temperature varying  $\eta$  and taking for  $\lambda_\perp$  value,  $\lambda_\perp = 5 \times 10^{-5}$ . The results obtained are given in Table II and are also shown in Fig. 3.

 TABLE II. The Néel temperature ( $T_N$ ) dependence on  $\eta$  for  $\lambda_\perp = 5 \times 10^{-5}$  in tetragonal phase.

$\eta$	$5 \times 10^{-2}$	$10^{-2}$	$10^{-3}$	$5 \times 10^{-4}$	$10^{-4}$	$10^{-5}$	$10^{-6}$	$10^{-7}$	$10^{-8}$	$10^{-10}$	0
$T_N^{2D}$ (K)	734.8	494.1	330.1	299.6	246.5	196.6	163.4	139.8	122.2	97.6	0
$T_N^{3D}$ (K)	734.8	494.1	330.1	299.6	246.5	196.6	163.4	139.8	122.2	97.6	0


 FIG. 3. The Néel temperature ( $T_N$ ) dependence on  $\eta$  for  $\lambda_\perp = 5 \times 10^{-5}$  in tetragonal phase.

The results from Table II show that in the 2D case  $T_N$  decreases when  $\eta$  becomes smaller and finally becomes 0 for  $\eta = 0$  which is expected due to the Mermin-Wagner theorem. The results obtained for the 3D case are almost indistinguishable from those obtained for the 2D case (Table II, Fig. 3), also showing that the Néel temperature for the spin isotropic 3D antiferromagnet becomes 0. The divergency of the quantity  $C$  given by Eq. (31) for  $\eta = 0$  is not only obtained numerically, but also can be ruled out analytically. In fact, in the center of the 3D AF Brillouin zone ( $|\vec{k}| \rightarrow 0$ ), this quantity is defined by the following integral:

$$C \approx \frac{1}{(2\pi)^3} \int_0^{k_0} k^2 dk \int_0^\pi \sin \theta d\theta \times \int_0^{2\pi} \frac{1}{k^2 \sin^2 \theta [1 - 3\lambda_2 + \lambda_\perp / 2 \sin 2\varphi]} d\varphi. \quad (34)$$

From this expression it is obvious that the integration over  $\theta$  is responsible for the divergency of  $C$ :

$$C \sim \int_0^\pi \frac{\sin \theta}{1 - \cos^2 \theta} d\theta \rightarrow \infty. \quad (35)$$

This fact appears to be the consequence of the Tyablikov approximation, which, itself, is in the agreement with the Mermin-Wagner theorem. One should notice that the Mermin-Wagner theorem offers strict result only for one and two dimensions, so our result does not contradict this theorem.

We have also calculated the Néel temperature for the ferromagnetic NNN-interaction, using for the parameters  $J$  and  $J_2$  values given in Ref. 1:  $J = 104 \pm 4$  meV,  $J_2 = -18 \pm 3$  meV. The obtained results also give the very weak de-

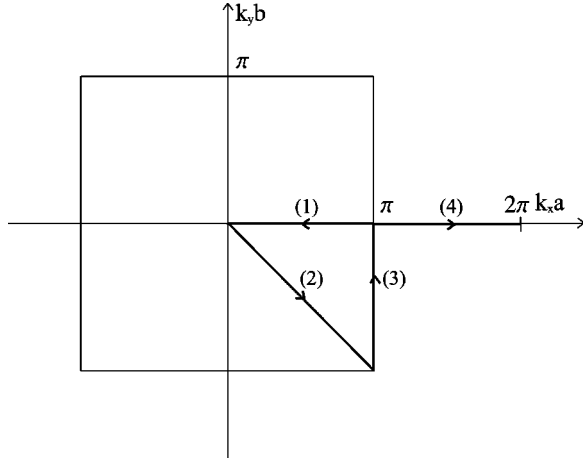


FIG. 4. The 2D AF Brillouin zone for the orthorhombic phase together with the selected path corresponding to that considered for the tetragonal structure.

pendence on the interlayer coupling, but show that the Néel temperatures close to the experimental value can be obtained only for  $\eta \approx 10^{-6}$ . For  $\eta \approx 10^{-3}$ , the obtained values for  $T_N$  were higher than 500 K. Hence, these results show that ferromagnetic NNN interaction can not yield the correct Néel temperature for any parameter set that could be characteristic for these systems.

In Appendix we review the complete calculation procedure for the orthorhombic phase of  $\text{La}_2\text{CuO}_4$  and compare the behavior of this phase to the tetragonal one, considering spin-wave spectrum and the Néel temperature.

Irkhin and Katanin<sup>14</sup> made a detailed comparison of the results obtained by linear spin-wave theory, self-consistent spin-wave theory, Tyablikov decoupling, and  $1/N$  expansion showing that only the last one leads to the reasonable value of  $T_N$ . However, a more detailed analysis of their equations shows that the calculation is based on the simple cubic structure, which is definitely an oversimplification.

#### IV. CONCLUSION

It can be seen from the literature concerning the problem of  $\text{La}_2\text{CuO}_4$  that there exists a variety of both models and parameters, which can fit more or less correctly the experimentally determined spin-wave spectrum. It is shown in this paper that the Néel temperature analysis is the one which introduces a strong restriction to the choice of models and parameters.

First, our analysis shows that NNN interaction has to be antiferromagnetic. Knowing that the ring exchange yields the effective ferromagnetic NNN interaction, this conclusion opens a dilemma if taking this specific type of exchange coupling is justified.

Second, the analysis of the Néel temperature shows that the in-plane spin anisotropy is much more significant than the three dimensionality (in agreement with the opinion of the authors of Ref. 9), since  $T_N$  depends rather weakly on the value of the interlayer coupling. This can be explained by the fact that either in tetragonal or in orthorhombic phase

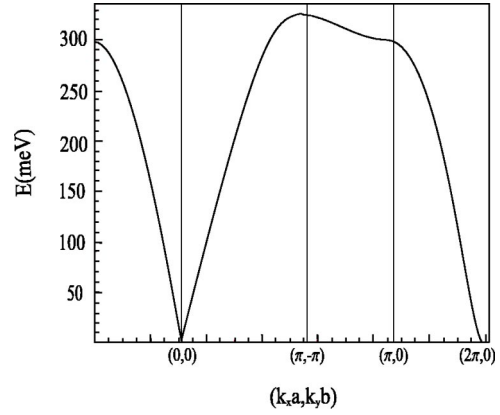


FIG. 5. Spin-wave dispersion in  $\text{La}_2\text{CuO}_4$  along the high symmetry directions in 2D AF Brillouin zone (for the orthorhombic phase). The solid line is the result of a fit to the spin-wave dispersion result (19) [with Eqs. (A1)–(A3)].

there are  $z_{\perp} = 8$  out-of-plane NN, which interact in different manners: four of them ( $z_{\perp}/2$ ) are coupled ferromagnetically and the other four antiferromagnetically. This practically produces the compensation of the terms involving interlayer coupling, as can be seen in expressions (28) and (29) for the tetragonal phase or in the analogous expressions written for the orthorhombic phase. Moreover, in the tetragonal phase (in our approximation) we obtain the zero value for the Néel temperature of the 3D spin isotropic antiferromagnet.

According to the Mermin-Wagner theorem, in order to explain AF long-range order at  $T \neq 0$  K in lanthanides, one needs either anisotropy or three dimensionality. Taking into account that the Hubbard Hamiltonian yields the in-plane spin isotropy, the importance of the in-plane spin anisotropy also raises the question whether the Hubbard Hamiltonian can be applied to these systems without any additional assumptions. It seems that this Hamiltonian is much more adequate to use in the (doped) superconductive phase, which, however, is questioned now by some recent results.<sup>15</sup>

Finally, we wish to point out that the values of all the parameters ( $J, J_2, \lambda_{\perp}, \eta$ ), which lead to the best fit of the spin-wave spectrum and the correct value of the Néel tem-

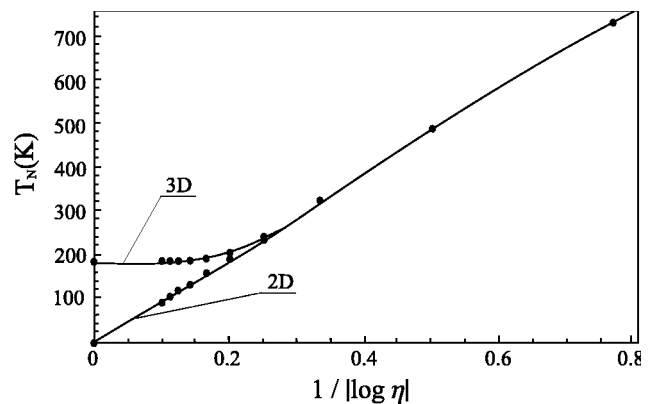


FIG. 6. The Néel temperature ( $T_N$ ) dependence on  $\eta$  for  $\lambda_{\perp}^{(1)} = 6 \times 10^{-5}$  and  $\lambda_{\perp}^{(2)} = 10^{-5}$  in orthorhombic phase, for the 2D and 3D case.

TABLE III. Néel temperature ( $T_N$ ) dependence on  $\lambda_{\perp}^{(1)}$  ( $\lambda_{\perp}^{(2)}$ ) for different  $\Delta\lambda_{\perp}=\lambda_{\perp}^{(1)}-\lambda_{\perp}^{(2)}$  and  $\eta=1.05\times 10^{-3}$  in orthorhombic phase.

		$\lambda_{\perp}^{(1)}$	$6\times 10^{-5}$	$1.5\times 10^{-4}$	$1.05\times 10^{-3}$	$1.005\times 10^{-2}$
	$10^{-5}$	$T_N$ (K)	333.0	333.0	333.1	333.2
		$\lambda_{\perp}^{(1)}$	$6\times 10^{-5}$	$1.5\times 10^{-4}$	$1.05\times 10^{-3}$	$1.005\times 10^{-2}$
$\lambda_{\perp}^{(1)}-\lambda_{\perp}^{(2)}$	$5\times 10^{-5}$	$T_N$ (K)	325.0	325.0	325.0	325.1
		$\lambda_{\perp}^{(1)}$	$2\times 10^{-4}$	$1.1\times 10^{-3}$	$1.01\times 10^{-2}$	$1.001\times 10^{-1}$
	$10^{-4}$	$T_N$ (K)	334.6	334.6	334.7	334.9

perature, are in a good agreement with the values most often cited in the literature.

### ACKNOWLEDGMENTS

This work was supported by the Serbian Ministry of Science and Technology, Project No. OI 1895.

### APPENDIX

As mentioned in Sec. I, the undoped  $\text{La}_2\text{CuO}_4$  crystallizes in the orthorhombic ( $Bmab$ ) phase<sup>4</sup> below the temperature  $T_{st}=530$  K. Therefore, we shall repeat the whole calculation, both for the spin-wave spectrum and the Néel temperature, for the orthorhombic phase of the system. In this phase, the magnetic cell is face-centered, characterized by the following lattice constants:  $a=5.338$  Å,  $b=5.406$  Å, and  $c=13.141$  Å.<sup>4,5</sup> The effective Hamiltonian of the system is given by Eq. (1), where the term representing Dzyaloshinsky-Moriya interaction is neglected, as explained in Sec. II.

Applying the spin Green function method, we obtain the spin-wave spectrum given by expression (19), where the quantities  $\Phi$  are given by Eqs. (8)–(12) and the quantities  $\gamma(\vec{q})$  in the orthorhombic phase have the following form:

$$\gamma_1(\vec{q}) = \cos\frac{q_x a}{2} \cos\frac{q_y b}{2}, \quad (\text{A1})$$

$$\gamma_2(\vec{q}) = \frac{1}{2}(\cos q_x a + \cos q_y b), \quad (\text{A2})$$

$$\gamma_3(\vec{q}) = \cos q_x a \cos q_y b, \quad (\text{A3})$$

$$\gamma_{\perp}^{aa}(\vec{q}) = \gamma_{\perp}^{bb}(\vec{q}) = \cos\frac{q_z c}{2} \cos\frac{q_y b}{2}, \quad (\text{A4})$$

$$\gamma_{\perp}^{ab}(\vec{q}) = \gamma_{\perp}^{ba}(\vec{q}) = \cos\frac{q_z c}{2} \cos\frac{q_x a}{2}. \quad (\text{A5})$$

To reproduce the spin-wave spectrum, we consider the 2D Brillouin zone shown in Fig. 4, together with the selected path corresponding to that considered for the tetragonal structure.

Here, for instance, point  $(\pi; 0)$  corresponds to the point  $(\frac{\pi}{2}; \frac{\pi}{2})$  in the tetragonal 2D Brillouin zone, point  $(\pi; -\pi)$  corresponds to  $(\pi; 0)$ , and so on. Taking this into account, we obtain the spin-wave spectrum (Fig. 5) similar to the previous one.

We have also calculated the Néel temperature for this phase, using expression (30), where  $C$  is now given by

$$C = \frac{1}{N} \sum_{\vec{k}} \frac{1 + \eta + (\lambda_{\perp}^{(1)} - \lambda_{\perp}^{(2)}) - \lambda_2 [2 - \gamma_2(\vec{k}) - \gamma_3(\vec{k})] + \lambda_{\perp}^{(2)} \gamma_{\perp}^{aa}(\vec{k})}{\{1 + \eta + (\lambda_{\perp}^{(1)} - \lambda_{\perp}^{(2)}) - \lambda_2 [2 - \gamma_2(\vec{k}) - \gamma_3(\vec{k})] + \lambda_{\perp}^{(2)} \gamma_{\perp}^{aa}(\vec{k})\}^2 - [\gamma_1(\vec{k}) + \lambda_{\perp}^{(1)} \gamma_{\perp}^{ab}(\vec{k})]^2}. \quad (\text{A6})$$

First, we calculated the Néel temperatures varying  $\lambda_{\perp}^{(1)} - \lambda_{\perp}^{(2)}$  and taking for the parameter  $\eta$  the value  $\eta \approx 10^{-3}$ , which gives the best agreement with the experimental value for  $T_N$ . The obtained results are shown in Table III.

It can be seen from Table III that the best agreement with the experimental value is obtained for  $\lambda_{\perp}^{(1)} - \lambda_{\perp}^{(2)} = 5 \times 10^{-5}$ , as suggested in Ref. 4. One can also notice that the results differ very little from those for the tetragonal phase, so the conclusions given in Sec. III con-

TABLE IV. The Néel temperature ( $T_N$ ) dependence on  $\eta$  for  $\lambda_{\perp}^{(1)} = 6 \times 10^{-5}$  and  $\lambda_{\perp}^{(2)} = 10^{-5}$  in orthorhombic phase.

$\eta$	$5 \times 10^{-2}$	$10^{-2}$	$10^{-3}$	$10^{-4}$	$10^{-5}$	$10^{-6}$	$10^{-7}$	$10^{-8}$	$10^{-9}$	$10^{-10}$	0
$T_N^{2D}$ (K)	726.6	485.2	321.7	239.1	190.1	157.8	134.8	117.7	104.5	93.9	0
$T_N^{3D}$ (K)	726.6	485.6	322.6	243.5	206.2	192.5	188.1	186.7	186.2	186.1	186

cerning the dependence on the interlayer coupling are still valid.

Next, we calculated the Néel temperatures varying the parameter  $\eta$ . The results are shown in Table IV and in Fig. 6.

The results show that in the 2D case the behavior of the

orthorhombic phase is similar to the tetragonal phase. In the 3D case, yet, we notice that when  $\eta$  becomes smaller,  $T_N$  converges to the value  $T_N \approx 186$  K, which is the consequence of the fact that the quantity  $C$  in this phase [Eq. (A6)] does not diverge for  $\eta=0$ , as can be seen from the following expression:

$$C(|\vec{k}| \rightarrow 0) \simeq \frac{4}{(2\pi)^3} \int_0^{k_0} k^2 dk \int_0^\pi \sin \theta d\theta \int_0^{2\pi} \frac{1}{k^2 [\cos^2 \theta (\lambda_\perp^{(1)} - \lambda_\perp^{(2)}) + \sin^2 \theta (1 - 6\lambda_2 + \lambda_\perp^{(1)} \cos^2 \varphi - \lambda_\perp^{(2)} \sin^2 \varphi)]} d\varphi. \quad (\text{A7})$$

It is obvious that this integral diverges only if  $\lambda_\perp^{(1)} = \lambda_\perp^{(2)}$ , which is actually the case in the tetragonal phase.

\*Email address: milica@unsim.ns.ac.yu

<sup>1</sup>R. Coldea, S.M. Hayden, G. Aeppl, T.G. Perring, C.D. Frost, T.E. Mason, S.W. Cheong and Z. Fisk, Phys. Rev. Lett. **86**, 5377 (2001).

<sup>2</sup>E. Dagotto, Rev. Mod. Phys. **66**, 763 (1994).

<sup>3</sup>C.J. Peters, R.J. Birgeneau, M.A. Kastner, H. Yoshizawa, J. Endoh, J. Tranquada, G. Shirane, Y. Hidaka, M. Oda, M. Suzuki, and T. Murakami, Phys. Rev. B **37**, 9761 (1988).

<sup>4</sup>R.J. Birgeneau, M. Greven, M.A. Kastner, Y.S. Lee, B.O. Wells, Y. Endoh, K. Yamada, G. Shirane, cond-mat/9903124 (unpublished).

<sup>5</sup>N.M. Plakida, *High-Temperature Superconductors* (Springer-Verlag, Berlin, 1995).

<sup>6</sup>A.A. Katanin and A.P. Kampf, cond-mat/0111533 (unpublished).

<sup>7</sup>S.V. Tyablikov, *The Methods in the Quantum Theory of Magnetism* (Plenum Press, New York, 1967).

<sup>8</sup>H.B. Callen, Phys. Rev. **130**, 890 (1963).

<sup>9</sup>J. Rossat-Mignod, L.P. Regnault, P. Bourges, P. Burlet, C. Vettier, and J.Y. Henry, in *Frontiers in Solid State Sciences: Magnetism and Superconductivity* (World Scientific, Singapore, 1994).

<sup>10</sup>N.M.R. Peres and M.A.N. Araújo, Phys. Rev. B **65**, 132404 (2002).

<sup>11</sup>M. Takahashi, J. Phys. C **10**, 1289 (1977).

<sup>12</sup>J.F. Annett, R.M. Martin, A.K. McMahan, and S. Satpathy, Phys. Rev. B **40**, 2620 (1989).

<sup>13</sup>B. Keimer, N. Belk, R.J. Birgeneau, A. Cassanho, C.Y. Chen, M. Greven, M.A. Kastner, A. Aharony, Y. Endoh, R.W. Irwin, and G. Shirane, Phys. Rev. B **46**, 14034 (1992).

<sup>14</sup>V.Y. Irkhin and A.A. Katanin, Phys. Rev. B **55**, 12318 (1997).

<sup>15</sup>I. Božović, G. Logvenov, M.A.J. Verhoeven, P. Caputo, E. Goldobin, and T.H. Geballe, Nature (London) **422**, 873 (2003).